

Metabolic support of Na⁺ pump in apically permeabilized A6 kidney cell epithelia: role of creatine kinase

MARIA LOURDES GUERRERO,¹ JÖRG BERON,² BENJAMIN SPINDLER,²
PETER GROSCURTH,³ THEO WALLIMANN,¹ AND FRANÇOIS VERREY²
Institutes of ²Physiology and ³Anatomy, University of Zürich, CH-8057 Zurich;
and ¹Institute for Cell Biology, Swiss Federal Institute of Technology,
CH-8093 Zurich, Switzerland

Guerrero, Maria Lourdes, Jörg Beron, Benjamin Spindler, Peter Groscurth, Theo Wallimann, and François Verrey. Metabolic support of Na⁺ pump in apically permeabilized A6 kidney cell epithelia: role of creatine kinase. *Am. J. Physiol.* 272 (*Cell Physiol.* 41): C697–C706, 1997.—The contribution of ATP-generating systems to Na⁺ pump (Na⁺-K⁺-ATPase) function was studied in *Xenopus laevis* A6 kidney epithelia apically permeabilized with digitonin. The ouabain-inhibitable Na⁺ pump current (*I_p*) was measured in the presence of otherwise impermeant inhibitors and/or substrates at Na⁺ and K⁺ concentrations that allowed near-maximal pump function. Confocal fluorescence microscopy after apical addition of sulfosuccinimidobiotin (molecular weight of 443) showed that all cells were permeabilized. Less than 15% of the endogenous lactate dehydrogenase and creatine kinase (CK) were released into the apical medium. The *I_p* was ~5 μA/cm² in the presence of D-glucose. Blocking glycolysis with 2-deoxy-D-glucose or oxidative phosphorylation with antimycin A decreased it by ≥50%. Exogenously added ATP prevented these decreases fully or partially, respectively. Two CK isoforms were detected, one likely being mitochondrial and the other corresponding to mammalian B isoform of CK. Phosphocreatine partially restored Na⁺ pump activity during inhibition of either ATP synthesis pathway. In conclusion, the ATP used by Na⁺ pumps of apically digitonin-permeabilized A6 epithelia is generated to a similar extent by glycolysis and oxidative phosphorylation. The CK system can partially support the ATP supply to the Na⁺ pumps.

epithelial sodium transport; sodium-potassium-adenosinetriphosphatase; sodium pump current; adenosine 5'-triphosphate; digitonin

THE DISTAL PART OF THE nephron is the site of the final adjustment of urinary Na⁺ excretion. Hormones and local factors act at this level by controlling the rate of Na⁺ reabsorption over a large range. The transport of Na⁺ across these epithelia is transcellular. For instance, at the level of collecting duct principal cells or cultured A6 cell epithelia, Na⁺ enters the cells via the apical epithelial Na⁺ channel and is extruded basolaterally by the Na⁺ pump (Na⁺-K⁺-ATPase). The Na⁺ pump also provides the driving force for apical Na⁺ influx and for the transport of other inorganic and organic substances (16).

The large and rapid changes in Na⁺ transport rate across distal nephron epithelia imply that Na⁺ pumps are able to pump at very different rates. This is achieved, on the one hand, by the intrinsic kinetic properties of this transport protein (2, 35) and, on the other hand, by the regulation of its function and of its cell-surface expression (4, 9, 35). Changes in Na⁺

pumping rate also require equivalent changes in ATP availability at the level of the Na⁺ pumps. Experiments addressing the question of the metabolic pathways involved in the production of ATP have been performed on dissected tubular segments. Glucose has been shown to be the most effective substrate for ATP maintenance in distal nephron (31) and for Na⁺ transport support in the cortical collecting duct (25). Correspondingly, the distal part of the nephron was shown to express high levels of hexokinase activity (32). It has to be mentioned that the latter experiments on ATP content and Na⁺ transport were performed on intact cells, such that the intracellular Na⁺ concentration was not controlled and might have differentially limited the Na⁺ pump activity. In the case of A6 cells, a study performed on cell suspensions indicates that the ATP used by the Na⁺ pump is preferentially produced by glycolysis rather than by oxidative metabolism (20). This finding suggests that ATP produced by membrane-bound glycolytic enzymes could be preferentially used by the Na⁺ pump, analogous to the situation found in erythrocytes (24, 27). However, in this case, suspended A6 cells taken from dish cultures were studied, which certainly differ from differentiated cells within the epithelial structure.

The creatine kinase-phosphocreatine (CK-PCr) system is known to play an important role as a high-energy phosphate store, buffer, and shuttle in cells with fluctuating and/or high-energy requirements, e.g., in skeletal and cardiac muscle cells, neurons, spermatozoa, etc. In these cells, different CK isoenzymes are specifically localized at sites of ATP generation and utilization (36, 38). Interestingly, higher CK activity and PCr content were found in distal tubules compared with more proximal segments of the nephron. Furthermore, the PCr level was acutely decreased only in distal tubules when the kidney was submitted to a brief ischemia (collecting duct was not included in this study) (1). Immunological studies have also supported the notion that CK is more prominent in distal tubular segments than in proximal ones (10, 14), and both the cytosolic B isoform of CK (B-CK) and mitochondrial CK have been found in mammalian kidney (10, 26). In kidney tubular cells, it is expected that the CK system provides energy for the Na⁺ pump (36). In this respect, experiments performed on cardiac muscle, electric organ, and gill cells have shown that CK can be functionally coupled to the Na⁺ pump, indicating that, in these cases, the Na⁺ pump preferentially uses ATP produced by colocalized CK (5, 19, 30, 36). A direct assessment of the role of PCr in conjunction with the function of the

Na^+ pump has not yet been performed in kidney tubular cells and, in particular, in distal nephron cells.

We describe here the use of apically digitonin-permeabilized A6 cell epithelia cultured on filters to test the contribution of different ATP-generating systems on the Na^+ transport function. This approach allows the introduction of otherwise impermeant substrates into the cells and the direct measurement of their impact on the activity of the Na^+ pump measured as Na^+ pump current (I_p) at a controlled intracellular Na^+ concentration. We attempt to characterize the CK activity present in A6 cells and its functional role in supporting the Na^+ pump function.

METHODS

Cell culture. A6 cells (cell line derived from the distal nephron of *Xenopus laevis*) from the A6-C1 subclone (passages 108–122) were cultured on polycarbonate filters (Transwell, 0.4 μm pore size, 4.7 cm^2 , Costar) coated with a thin collagen layer, as previously described (3). Experiments were performed on epithelia cultured for a total of 15–22 days, the first 10 days in medium containing bicarbonate and 10% fetal bovine serum and then in serum- and bicarbonate-free medium.

Apical permeabilization and measurement of I_p . Transepithelial electrical measurements were performed as previously described on monolayers cultured on Transwell filtercups in a modified Ussing chamber with an automatic voltage-clamp device connected either to a dual-channel recorder or to a MacLab/4e data recording unit, with the use of the Chart software (AD Instruments, Castel Hill, Australia) (33).

Before use, filter cultures were briefly washed three times on both sides in the original culture wells with apical and basolateral buffer, respectively. The apical buffer contained (in mM) 40 sodium gluconate, 53 potassium gluconate, 0.1 calcium gluconate, 2 MgCl_2 , 1 K_2HPO_4 , and 25 *N*-2-hydroxyethylpiperazine-*N'*-2-ethanesulfonic acid (HEPES), pH adjusted to 7.4 with NaOH (~8.5 mM). The basolateral buffer contained (in mM) 90 sodium gluconate, 3 potassium gluconate, 1 calcium gluconate, 2 MgCl_2 , 1 K_2HPO_4 , 25 HEPES, and 5 mM BaOH [to block K^+ channels (2)] (final pH 7.4). Both buffers were supplemented with 5 or 20 mM of either D-glucose or 2-deoxy-D-glucose. The filtercups containing 2 ml apical buffer were then transferred to the Ussing chamber (containing 7 ml basolateral buffer) and maintained in short-circuit configuration (voltage clamped at 0 mV). After a preincubation period of ~3 min, digitonin was added to the apical buffer at a final concentration of 10 μM (from a 20 mM stock in H_2O ; Ref. 6) together with ADP (1 mM, stock of 1 M in H_2O) by mixing them with a volume of apical buffer, which was taken and added back without interrupting the voltage clamp. The spontaneous potential difference was measured 10–12 min after digitonin addition ($V_{\text{TE}12'}$), and the voltage clamp was set to that level. One of the external substrates [MgATP, neutralized with NaOH; PCr; phosphoarginine; phosphoenolpyruvate (PEP); or NaCl (alternatively MgCl_2)] was added to the apical buffer by the same procedure from 1 M stock solutions. When required, antimycin A (a blocker of oxidative phosphorylation) was added 30 min before the experiment was started on both sides of the epithelium into the culture medium to a final concentration of 10 μM (stock solution 10 mM in ethanol; Ref. 22). The treatment was continued during the wash and permeabilization procedures. The transepithelial resistance (R_{TE}) was monitored at irregular intervals by measuring the current change induced by a

1-mV voltage step. Finally, ouabain (100 μM) was added to the basolateral compartment (without interrupting the voltage clamp) 20 min after the beginning of permeabilization. The decrease in current during the first minute after ouabain addition was taken as I_p .

Actual tracings obtained with this setup are displayed in Fig. 1. The results shown in the bar graphs (see Figs. 6–8) represent means and standard errors obtained from n independent experiments. In each of these experiments all conditions were tested on one to four filters. Variations between conditions were tested by analysis of variance, and the significance of the difference between pairs was determined with the Student-Newman-Keuls posttest. Student's *t*-test was applied where indicated.

Permeability test to sulfo-NHS-biotin. The permeabilization was performed as described above for I_p measurements with buffers containing D-glucose. Sulfo-NHS-biotin (Pierce, Rockford, IL) was added apically 10 min after the beginning of permeabilization to a final concentration of 100 $\mu\text{g}/\text{ml}$ (from a 1 mg/ml stock made in H_2O and kept frozen in liquid nitrogen). After 10 min, the epithelia were briefly washed twice with apical and basolateral buffers. To the 1 ml buffer present on each side of the epithelium, 1 ml of a 3% paraformaldehyde-2% sucrose solution made in K^+ -piperazine-*N,N'*-bis(2-ethanesulfonic acid) (PIPES) buffer [80 mM PIPES (pH 6.8), 2 mM MgCl_2 , and 5 mM ethylene glycol-bis(β -aminoethyl ether)-*N,N,N',N'*-tetraacetic acid] was added for 30 min at room temperature. The filters were washed three times with phosphate-buffered saline (PBS), cut into small pieces, treated for 3 min with 0.1% Triton X-100 in PBS, and washed again twice with PBS. Incubation with streptavidin-Texas red (1:50 in PBS) (Amersham, Little Chalfont, England) was done between two 30- μl drops in a humid box for 2 h at room temperature. After three washes with PBS, filter pieces were mounted on glass slides and observed with a confocal laser microscope (Zeiss LSM III). Three to four serial optical sections were taken from each specimen in the central part of the cells at 0.6- μm -depth increments and digitally superimposed. Except for proper adjustment of contrast and brightness, no image processing was performed.

Measurement of lactate dehydrogenase and CK activity and release. The epithelia were treated exactly as for the measurements of the I_p . After addition of ouabain to the basolateral medium, the apical buffer was collected, and a protease inhibitor cocktail was added (leupeptin, pepstatin, and aprotinin at a final concentration of 2 $\mu\text{g}/\text{ml}$), frozen in liquid nitrogen, and stored at -70°C . The cell-associated enzymes were extracted with a buffer containing 1% Triton X-100 and 0.4% sodium deoxycholate as described for Western blotting in Ref. 3 and also frozen. Lactate dehydrogenase (LDH) and CK activities were determined according to published procedures (13, 37). For the enzyme release experiments, no significant difference was observed between results obtained from filters incubated in buffer containing D-glucose or 2-deoxy-D-glucose, such that the values were pooled. Measurements of the specific activity of CK were done on fresh cells. Proteins were determined with a commercial kit (Bio-Rad, Hercules, CA).

Separation of CK isoforms of intact and fractionated A6 cells by native cellulose polyacetate electrophoresis. The cell extracts, prepared as for the enzyme activity determinations, were separated by cellulose polyacetate electrophoresis for 1 h at 200 V as described previously, and the CK activity was visualized by the overlay gel technique as described (39). For fractionation, A6 epithelia (7 filters, total of 34 cm^2) were first washed with homogenization buffer containing (in mM) 180 mannitol, 60 sucrose, 10 HEPES, 0.2 EDTA, and 5 β -mercap-

toethanol, adjusted to pH 7.4. The cells were then scraped in 350 μl of the same buffer and disrupted with 10 strokes of a Teflon-glass homogenizer set at 2,500 revolutions/min. Cells and debris were pelleted for 5 min at 20,000 g in a S120AT2 rotor (Sorvall, DuPont, Newtown, CT). The pellet was resuspended in the same volume, and the homogenization procedure was repeated. The homogenate was centrifuged at 1,100 g for 2 min, and the supernatant was submitted to another centrifugation at 20,000 g for 5 min. The pellet, which was washed once more, represents the membrane fraction analyzed in Fig. 4, lane 7. The cytosolic fraction shown in lane 6 (see Fig. 4) corresponds to the pooled supernatants of the 20,000 g centrifugations, which were cleared from remaining membranes by a 200,000 g centrifugation (20 min).

Northern blotting. Poly(A)⁺ RNA was prepared from filter-cultured A6 cells by the proteinase K method (11), separated on an agarose-formaldehyde gel, and transferred to a nylon membrane (GeneScreen, DuPont-New England Nuclear). The blots were probed at high stringency with ³²P-labeled (oligolabeling kit, Pharmacia, Brussels, Belgium) cDNA fragments of type III [muscle-specific cytosolic CK (M-CK)] and IV (ubiquitous cytosolic B-CK) *X. laevis* CK (28). The radioactivity was visualized with the phosphorimager system (Molecular Dynamics, Sunnyvale, CA).

RESULTS

Measurement of the I_P in A6 epithelia apically permeabilized with digitonin. To permeabilize the apical membrane of A6 cells to ions and metabolic substrates, digitonin was added in the apical buffer of epithelia placed in a modified Ussing chamber at 26°C in short-circuit configuration (voltage clamped at 0 mV; Fig. 1A). Because of the permeabilization of the apical membrane, the R_{TE} decreased within 10 min from $4,900 \pm 380 \Omega \cdot \text{cm}^2$ (before permeabilization) to $1,360 \pm 130 \Omega \cdot \text{cm}^2$ (means of controls, $n = 14$) (Table 1). $V_{TE(12)}$ was then measured, and the voltage clamp was adjusted to the measured value. The R_{TE} remained generally stable during the remainder of the experiment in the continuous presence of digitonin. The I_P was measured 20 min after the beginning of permeabilization by the addition of ouabain. The I_P values obtained in the control situation were similar to those previously obtained with A6 cells apically permeabilized with amphotericin B [mean of controls of 5.2 $\mu\text{A}/\text{cm}^2$ in this study vs. 4.5 to 7.5 $\mu\text{A}/\text{cm}^2$ in amphotericin-treated epithelia (2)]. This suggests that the spatial arrangement of

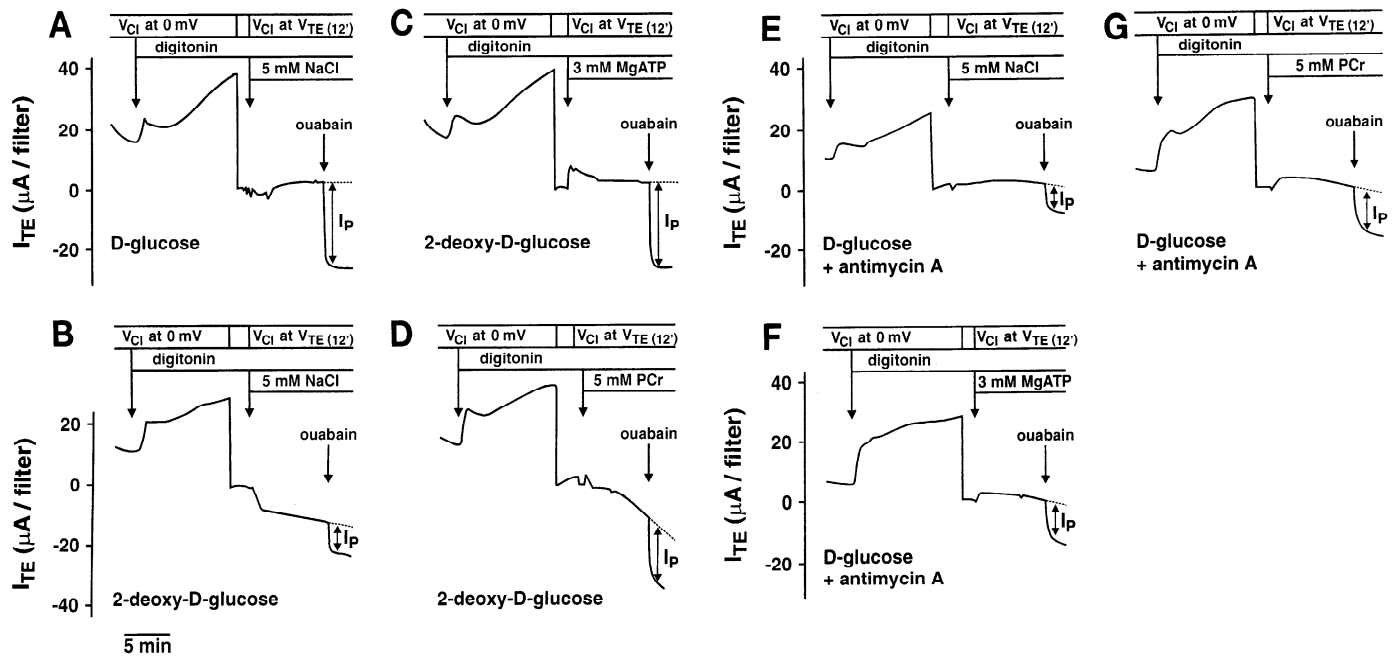


Fig. 1. Measurement of Na^+ pump current (I_P) in apically digitonin-permeabilized A6 epithelia. Recordings of transepithelial current (I_{TE}) from filters incubated in buffer supplemented with 5 mM of D-glucose, deoxy-D-glucose, or D-glucose + antimycin A (see METHODS). After a brief equilibration period, 10 μM digitonin (together with 1 mM ADP) was added to apical buffer where indicated. Holding potential of voltage clamp (V_{CI}) was reset 10–12 min after permeabilization was started from 0 mV (measurement of the short-circuit current) to spontaneous transepithelial potential difference [$V_{TE(12)}$], i.e., I_{TE} set to 0 μA]. Additional substrates or NaCl was added 12 min after permeabilization was started to apical buffer, and I_P was inhibited 8 min later by addition of 100 μM ouabain. Note that for each condition the shape of the current trace after substrate addition was more variable between experiments than amount of ouabain-inhibitable current (I_P). A: control epithelium incubated in buffers containing 5 mM D-glucose. NaCl (5 mM) was added instead of a substrate. B: inhibition of glycolysis (and progressive depletion of substrate for mitochondrial ATP production) by incubation in buffer containing 2-deoxy-D-glucose. NaCl (5 mM) did not prevent the decrease in I_P . C: inhibition of glycolysis as in B. Decrease in I_P prevented by addition of 3 mM MgATP. D: inhibition of glycolysis as in B. Decrease in I_P partially prevented by addition of 5 mM phosphocreatine (PCr). E: inhibition of oxidative phosphorylation with 10 μM antimycin A. NaCl (5 mM) did not prevent the decrease in I_P . F: inhibition of oxidative phosphorylation as in E. Decrease in I_P partially prevented by addition of 3 mM MgATP. G: inhibition of oxidative phosphorylation as in E. Decrease in I_P partially prevented by addition of 5 mM PCr.

Table 1. *Effect of apical permeabilization with digitonin on transepithelial electrical parameters and effect of inhibitors of endogenous ATP synthesis on the Na^+ pump current*

	Inhibition of Glycolysis		Inhibition of Oxidative Phosphorylation	
	D-Glucose	2-Deoxy-D-glucose	D-Glucose	D-Glucose + antimycin
I_{TE} before digitonin, $\mu\text{A}/\text{cm}^2$	2.24 ± 0.29	1.93 ± 0.26	1.99 ± 0.25	$1.37 \pm 0.15^*$
R_{TE} before digitonin, $\Omega \cdot \text{cm}^2$	$5,090 \pm 520$	$5,790 \pm 470$	$4,720 \pm 580$	$5,140 \pm 380$
R_{TE} 10 min after digitonin, $\Omega \cdot \text{cm}^2$	$1,660 \pm 200$	$1,590 \pm 220$	$1,060 \pm 43$	$1,040 \pm 50$
V_{TE} 12 min after digitonin, mV	12.9 ± 2.3	10.1 ± 1.6	8.95 ± 0.88	$6.86 \pm 0.67^*$
I_{P} 20 min after digitonin, $\mu\text{A}/\text{cm}^2$	5.81 ± 0.76	$2.17 \pm 0.27^\dagger$	4.67 ± 0.27	$2.1 \pm 0.19^\ddagger$

Values are means \pm SE from 7 independent experiments (control and test filters). I_{TE} , transepithelial current (measured at a time at which epithelia were voltage clamped at 0 mV such that the measured I_{TE} corresponded to the short-circuit current); R_{TE} , transepithelial resistance; V_{TE} , transepithelial potential difference; I_{P} , Na^+ pump current. Significance of differences between test and D-glucose values was tested with paired two-tailed *t*-tests: * $P < 0.05$, $^\dagger P < 0.01$, $^\ddagger P < 0.001$.

glycolytic enzymes is maintained so as to allow the glycolysis to proceed in spite of the apical permeabilization with digitonin. Using the number of ouabain-binding sites determined in a previous study (3), one can calculate that this I_{P} corresponds to ~ 60 cycles/s multiplied by the pump unit.

Apical permeability of digitonin-treated cells to exogenous substrates and release of endogenous enzymes. A hydrophilic succinimidyl derivative of biotin (sulfo-NHS-biotin, molecular weight of 443, Pierce) was used as a

probe to visualize the permeability of the apical membrane of digitonin-treated A6 cells to molecules with a size in the range of that of substrates such as ATP. Permeabilization was as for the electrophysiological experiments, and sulfo-NHS-biotin was added apically, as were the test substrates (see METHODS). The diffusion of this molecule into the cells and its covalent binding to cellular proteins were revealed with fluorescent streptavidin and confocal fluorescence microscopy. Figure 2 shows that, in contrast to the untreated monolayer, all cells of the digitonin-treated monolayer were similarly stained in the perinuclear region. This indicated that the pores produced by digitonin in the apical membrane were, in all cells, sufficiently numerous and large to allow an efficient diffusion of sulfo-NHS-biotin into such permeabilized cells.

To test the extent of endogenous proteins diffusing out of the cells after digitonin permeabilization, we determined the activity of LDH and CK that remained within the cells as well as that released into the apical medium (Fig. 3). When the apical membrane was treated with digitonin, $< 15\%$ of the cellular enzymes diffused into the apical medium during the course of the experiment (20 min from the beginning of permeabilization). The fact that only a rather small proportion of enzymes diffused out of the cells could be because of various reasons. First, the interaction of these enzymes with intact intracellular structures might largely retain them. Furthermore, in the case of CK, the subpopulation of the putative mitochondrial CK isoform (which represents the major fraction in these A6 cells) is not expected to diffuse out at all. Second, it is likely that the holes produced by digitonin are sufficiently small so as not to let large enzymes diffuse efficiently out of the cells or that the terminal web and/or a glycocalyx prevents their diffusion (8). An important conclusion from these results is that LDH, a large cytosolic enzyme that can play a role in the cytoplasmic production of ATP, mostly remained cell associated during the experiments. In contrast, it might be that a substantial

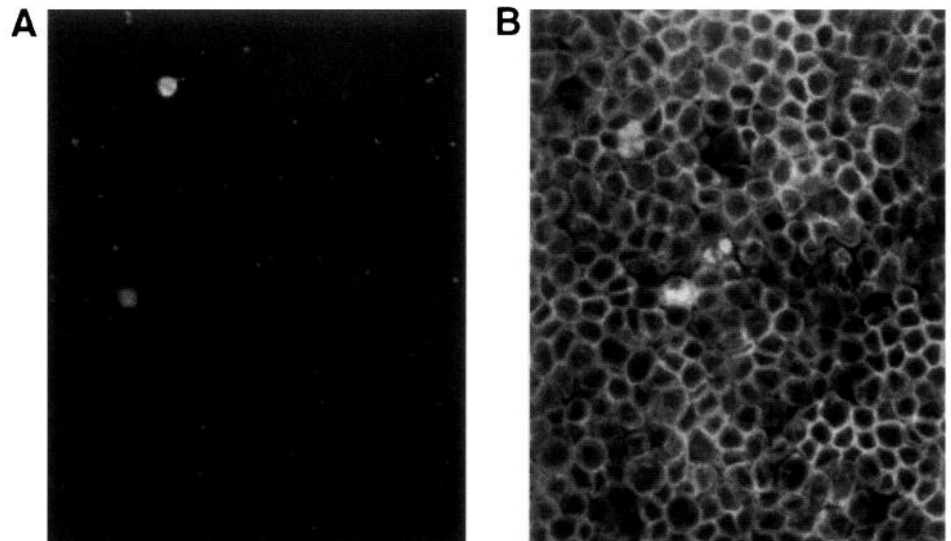


Fig. 2. Confocal fluorescence microscopy shows that all cells of apically digitonin-treated A6 epithelia are permeable to sulfo-NHS-biotin (molecular weight of 443). Vehicle (A) or digitonin (10 μM) (B) was added apically as in Fig. 1. Sulfo-NHS-biotin was added apically after 10 min, and incubation was continued for another 10 min. Epithelia were then washed, fixed, permeabilized with Triton X-100, and incubated with streptavidin-Texas red to visualize the covalently bound biotin.

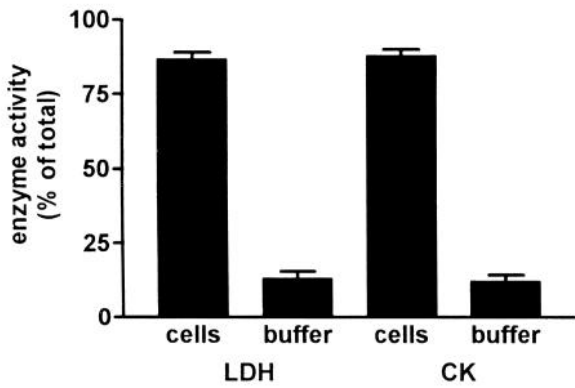


Fig. 3. Less than 15% of the cellular lactate dehydrogenase (LDH) and creatine kinase (CK) of apically digitonin-treated epithelia are released into the apical buffer. Epithelia were treated as for Fig. 1. LDH and CK activities were determined in the apical buffer and in the cell lysate. No LDH or CK activity was found in apical buffer when digitonin permeabilization was omitted. The results are expressed as percentage of total activity (buffer + cell lysate) and represent means and standard errors from 5 determinations.

part of the cytosolic CK isoform, which is the minor isoform in A6 epithelia (see below), could diffuse out of the cells. The identity of the diffusing CK isoenzyme was not assessed because of the low absolute amount of released activity.

Expression of CK in A6 cells. The specific activity of total CK in A6 epithelia was determined in three independent experiments and amounted to 0.99 ± 0.08 IU/mg proteins for control filters and 1.18 ± 0.02 IU/mg proteins for long-term aldosterone-treated filters, which express a high-Na⁺ transport activity. These values are

similar to those found in rat kidney [0.7, 1.2, and 0.6 IU/mg protein for total homogenate, medulla, and cortex, respectively (Guerrero and Wallimann, unpublished results), and 0.9 and 4.9 IU/mg protein for cortex and outer stripe and for inner stripe, respectively (10), but ~5-fold and 10-fold lower than those found in rat brain and skeletal muscle, respectively (Guerrero and Wallimann, unpublished observation)]. It does not appear that aldosterone, which stimulates Na⁺ transport in A6 epithelia via transcriptionally mediated mechanisms (34), induces a significant increase in the level of total A6 cell CK activity.

To characterize the CK activity found in A6 cells, we performed native cellulose polyacetate electrophoresis followed by visualization of the CK activity by the gel overlay technique (Fig. 4) (39). These experiments revealed the presence of two CK isoforms, a major one migrating toward the cathode and a less prominent one migrating toward the anode. The labeling of a third band migrating slowly toward the cathode was fully prevented by the addition of the adenylate kinase inhibitor P¹,P⁵-di(adenosine-5') pentaphosphate. The adenylate kinase appears as a very faint band in Fig. 4, lane 1, and appears as a prominent band in lane 2, where its enzymatic activity was revealed in the absence of PCr.

The relative intensity of the two CK bands was somewhat variable from experiment to experiment, indicating differential inactivation of the CK isoenzymes during sample preparation and/or electrophoresis. Thus the zymogram technique does not allow a precise quantitation of the relative amount of the two

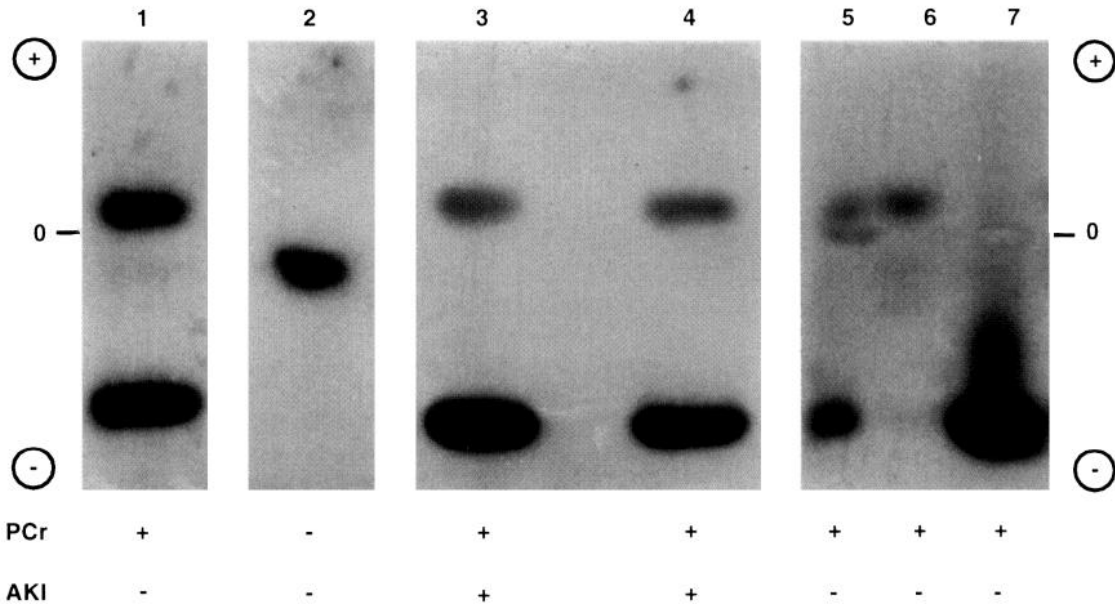


Fig. 4. Two CK isoforms, a cytosolic and a (putative) mitochondrial one, are revealed by native cellulose polyacetate electrophoresis of A6 cell lysate. Kinase activity was revealed after electrophoresis on cellulose polyacetate strips with the coupled enzyme gel overlay technique. Presence of CK substrate PCr and of adenylate kinase inhibitor (AKI) [0.3 mM P¹,P⁵-di(adenosine-5') pentaphosphate (AP5A); Ref. 39] is indicated. Lanes 1-3 correspond to epithelia cultured in control conditions; lane 4 corresponds to an epithelium treated for 24 h with aldosterone (10⁻⁶ M). Note the presence of adenylate kinase in A6 cells (lane 2). Lanes 5-7 show a fractionation experiment: lane 5 corresponds to total cell lysate and contains both isoforms plus adenylate kinase, lane 6 corresponds to a cytosolic fraction and contains only the anodic CK, and lane 7 is a membrane fraction (containing mitochondria) that contains only the cathodic CK, which presumably is a mitochondrial isoform.

isoforms. By analogy to the migration behavior of mammalian CK isoforms, it was tempting to speculate that the major CK band migrating toward the cathode represented a mitochondrial isoform and the minor band, which migrates slightly toward the anode, corresponded to a cytosolic one. To substantiate this assumption, we performed a crude fractionation of A6 epithelia that confirmed that the anodic band was indeed cytosolic (Fig. 4, lane 6), whereas the cathodic band remained membrane associated, as expected for a mitochondrial form (lane 7). Aldosterone appeared to have no effect on the expression of either isoform (lanes 3 and 4). We also compared the pattern of CK obtained with A6 epithelia on polyacetate electrophoresis with that obtained with native *X. laevis* tissues. As expected, the anodic band (corresponding to a cytosolic isoform) comigrated with the major band obtained with urinary bladder, a tissue in which the cytosolic isoform is expected to be the major one. The cathodic band comigrated with a prominent band found in brain, a tissue in which mitochondrial CK is expected to be highly expressed (data not shown).

To characterize further these isoforms, we used the two available *X. laevis* CK cDNAs that encode the type III muscle-specific and the type IV ubiquitous forms, respectively (28). The Northern blot analysis of A6 cell RNA shown in Fig. 5 indicated that the mRNA of the type IV isoform is strongly expressed in A6 cells and that this expression is not modified by an aldosterone treatment. This isoform corresponds to the mammalian B-CK, which also is the major cytoplasmic isoform expressed in rat kidney (10) as well as in avian kidney where no or only traces of mitochondrial CK are found (Guerrero, unpublished observation). In contrast, no signal was obtained on an identical Northern blot with the probe for the type III cytosolic M-CK (Fig. 5, right). In conclusion, A6 cell epithelia express two CK iso-

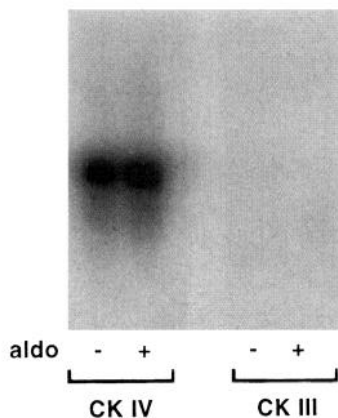


Fig. 5. A6 epithelia express the type IV CK [corresponding to mammalian B isoform of CK (B-CK)]. Northern blot analysis of poly(A)⁺ RNA extracted from A6 epithelia cultured in control conditions or for 24 h in presence of 10^{-6} M aldosterone. Radioactive probes of similar size and specific activity were prepared from the 2 available *Xenopus laevis* CK cDNAs encoding *X. laevis* cytosolic CK type IV (ubiquitous, corresponding to B-CK) and type III [muscle specific CK (M-CK)] (28). Note that cytosolic type IV (B-CK) mRNA is highly expressed and not induced by aldosterone, whereas cytosolic M-CK III mRNA is not detected in A6 cells.

forms: type IV, which generally appeared to be the minor one and which corresponds to the mammalian B-CK, and a major one, which is likely to be a mitochondrial form.

Inhibition of ATP-generating systems and compensation with exogenous substrates. Glycolysis and mitochondrial respiration were inhibited to test their respective contribution in fueling Na^+ pump function. These measurements were performed in the presence of controlled cytosolic Na^+ and basolateral K^+ concentrations, which allow the Na^+ pumps to function at a near-maximal rate (2, 15).

Glycolysis was inhibited by replacing D-glucose with 2-deoxy-D-glucose. This pseudosubstrate not only efficiently blocks glycolysis but also functions as an ATP sink, since it is a substrate of hexokinase forming 2-deoxy-D-glucose-6-phosphate. Furthermore, blocking the glycolysis also blocks the main source of substrate for the mitochondrial respiration. Figure 1B shows a tracing of the transepithelial current (I_{TE}) in the presence of 2-deoxy-D-glucose. Typically, the I_{TE} tended to decrease during the course of the experiment and the I_{P} measured 20 min after the initiation of permeabilization was on average 37% of that obtained in the presence of D-glucose (Table 1). In contrast, blocking oxidative phosphorylation with antimycin A yielded a stable I_{TE} that represented, on average, 45% of the control. Therefore, it can be deduced from this latter result that ~55% of the ATP used by the Na^+ pump at near-maximal pumping rate is produced by oxidative phosphorylation. The continuous decrease in I_{P} observed in the presence of 2-deoxy-D-glucose could be because of a progressive slowdown of the oxidative phosphorylation consecutive to the decrease in substrate available for the citric acid cycle.

To test the efficiency of the CK-PCr system and of other substrates in fueling the Na^+ pump, we first tried to block entirely the ATP production by adding inhibitors of both ATP-generating systems (2-deoxy-D-glucose plus antimycin A) and then adding substrates (i.e., ATP or PCr) concomitantly with permeabilization. This treatment, however, fully blocked Na^+ pump function in a way that was generally irreversible during the course of the experiment. It appears that regulatory changes or cellular damage caused by this treatment prevented the reactivation of the Na^+ pump function. Interestingly, this effect on Na^+ pump function was not preceded nor paralleled by a drop in R_{TE} as would have been expected on the basis of observations made in Madin-Darby canine kidney cells (21, 22).

The ability of exogenous substrates, which were added 12 min after the beginning of permeabilization, to rescue the Na^+ pump function was tested in epithelia treated with 2-deoxy-D-glucose or antimycin A to block either one of the ATP-production pathways. In the case of 2-deoxy-D-glucose, 3 mM MgATP fully restored the I_{P} (Figs. 1C and 6A). PCr (5 mM) was slightly less effective than 3 mM MgATP in supporting the I_{P} (difference not significant) (Fig. 6A). In particular, the I_{P} tended to be less stable (Fig. 1D), an observation that

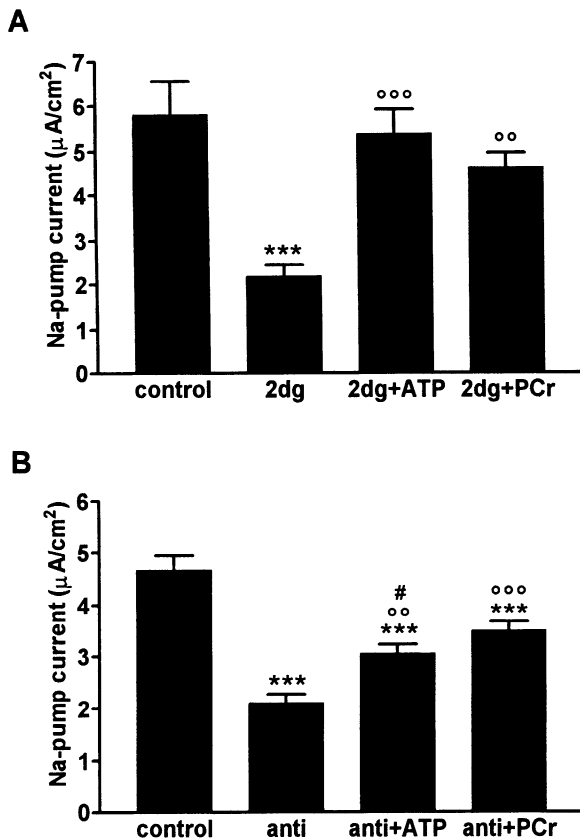


Fig. 6. Decrease in I_P produced by inhibitors of ATP-generating systems and compensation by exogenous substrates. Experimental protocol was as shown in Fig. 1. Results shown in *A* and *B* are each means \pm SE of 7 independent experiments. Significant differences of the test values vs. control values (** $P < 0.001$) and vs. 2-deoxy-D-glucose or antimycin A values (°° $P < 0.001$, ° $P < 0.01$) are indicated. *A*: inhibition of glycolysis (and progressive depletion of substrate for citric acid cycle). Permeabilization was in the presence of D-glucose (control) or 2-deoxy-D-glucose (2dg). After 12 min, 5 mM NaCl (control and 2dg), 3 mM ATP, or 5 mM PCr was added apically. Ouabain-sensitive transepithelial current (I_P) was measured 20 min after digitonin addition. *B*: inhibition of oxidative phosphorylation. Antimycin A (anti; 10 μ M) was added 30 min before permeabilization. Substrate addition and I_P measurement were as in *A*. I_P obtained with ATP (relative to control) in antimycin A vs. 2-deoxy-D-glucose-treated epithelia was significantly different ($\#P < 0.05$).

might be related to a progressive loss of cytosolic CK during the course of the measurements.

In contrast to the situation observed in 2-deoxy-D-glucose-treated epithelia, 3 mM MgATP only partially restored the Na⁺ pump function in antimycin A-treated epithelia (significantly less than in 2-deoxy-D-glucose-treated epithelia). In this case, however, PCr (5 mM) tended to be relatively more efficient than ATP (Fig. 6*B*). Concerning the concentrations of MgATP and PCr used, it should be noted that they were in the range expected for distal nephron cells (1) but that local concentrations at the level of the CK and the Na⁺ pump cannot be controlled.

Whether the effect of PCr was due to its role as substrate for CK was tested by using the phosphagen analog, phosphoarginine, which is not metabolized by CK. Figure 7 shows that phosphoarginine indeed had no effect on I_P , either in the case of 2-deoxy-D-glucose

or in the case of antimycin A-treated epithelia. This also demonstrates that the amphibian A6 cells do not contain arginine kinase.

As an alternative source of high-energy phosphate, 5 mM PEP was also added (Fig. 8). The hydrolysis of PEP by the endogenous pyruvate kinase not only produces ATP but also pyruvate, which is a substrate for mitochondrial respiration. Interestingly, PEP appeared to be as effective as PCr in supporting Na⁺ pump function under the conditions of oxidative phosphorylation inhibition. This indicates that the pyruvate kinase-PEP system was as effective as the CK-PCr system in providing ATP to the Na⁺ pump. As expected from its role as a substrate source for mitochondrial respiration, PEP was, in the case of glycolysis inhibition, more effective than PCr in restoring Na⁺ pump function. The similarity of the effects of endogenous CK and pyruvate kinase for supporting Na⁺ pump fueling corresponds to the observations made on plasma membrane Ca²⁺-ATPase fueling in smooth muscle cells (12).

DISCUSSION

Conditions for measurement of I_P in digitonin-permeabilized epithelia. Apically digitonin-permeabilized A6 cell epithelia represent a new experimental system in which the effect of otherwise impermeant

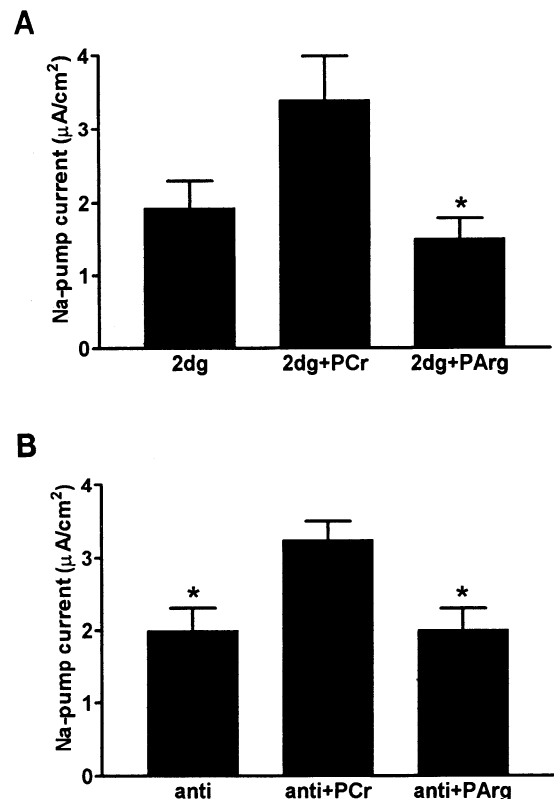


Fig. 7. Phosphoarginine (PArg), an analog of PCr, is not active as phosphagen. Experiments were performed as for Fig. 6. I_P was significantly smaller when PArg was added instead of PCr (* $P < 0.05$). *A*: inhibition of glycolysis with 2-deoxy-D-glucose. Bars represent means \pm SE from 5 independent experiments. *B*: inhibition of oxidative phosphorylation with antimycin A. Bars represent means \pm SE from 4 independent experiments.

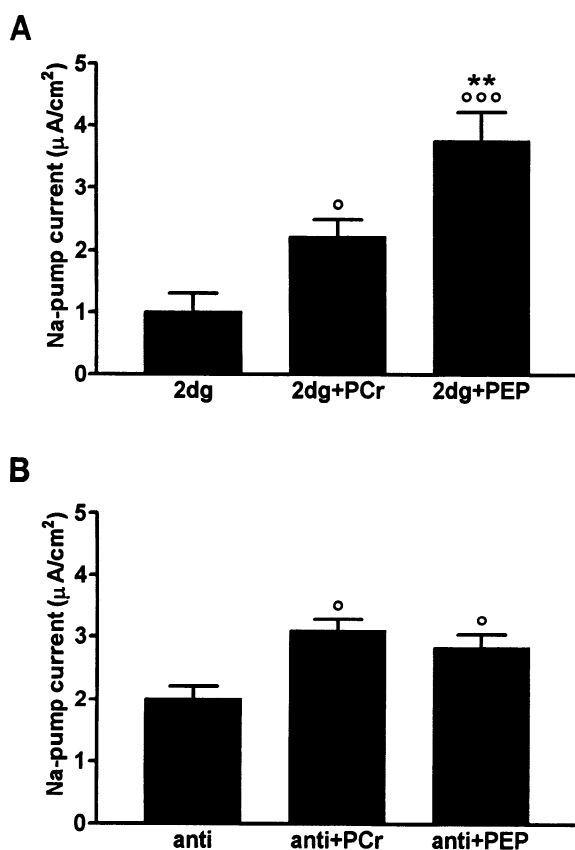


Fig. 8. Phosphoenolpyruvate (PEP) functions as phosphagen and substrate for the citric acid cycle. Experiments were performed as for Fig. 6. Bars represent means \pm SE from 6 independent experiments. *A*: inhibition of glycolysis with 2-deoxy-D-glucose. *B*: inhibition of oxidative phosphorylation with antimycin A. I_p of epithelia treated with 2-deoxy-D-glucose or antimycin A was significantly increased by the addition of PCr or PEP (* $P < 0.05$, *** $P < 0.001$). PEP supported a significantly higher I_p than PCr when glycolysis and not oxidative phosphorylation was blocked (** $P < 0.01$).

substances on the in situ function of Na^+ pumps can be directly measured. Because the aim of the present study was to test the role of ATP-generating systems in fueling the Na^+ pump, conditions in which the Na^+ transport would be limited by the ATP availability were designed. A few points concerning the experimental conditions are now discussed.

Asymmetric buffers were chosen to impose a workload on the Na^+ pump such that very low-ATP concentrations would not allow it to pump forward. In these conditions [2-fold Na^+ and 10-fold K^+ concentration gradients, mean potential difference of 9.7 ± 0.8 mV ($n = 28$, see Table 1)], the energy required per pump cycle amounted to ~ 190 meV, corresponding to 18.5 kJ/mol ATP, assuming the transport of three Na^+ out and two K^+ into the cell per cycle (7). It can be estimated that, in the presence of 1 mM each of ADP and P_i , thermodynamic equilibrium would in this case be reached at an ATP concentration of ~ 10 μM . Hence, low-micromolar concentrations of ATP would not suffice, from a thermodynamic point of view, for forward pumping by the Na^+ pump. It is not known to what extent the kinetics of ATP binding would limit the

function of the Na^+ pumps at such a low ATP concentration in A6 epithelia. In most systems, half-maximal activation of Na^+ pumps has been observed at around 0.2 mM ATP. However, biphasic activation curves and high (apparent)-affinity ATP-binding sites have also been reported, indicating that a substantial pumping rate could be possible, from a kinetic point of view, at micromolar ATP concentrations (7, 23).

From a previous study with amphotericin B-permeabilized cells, we can estimate that the cytosolic Na^+ concentration of 49 mM used in this study would allow for 90% of maximal Na^+ pump current ($I_{p\text{max}}$) (2) and from measurements in *Xenopus* oocytes that the basolateral K^+ concentration of 5 mM would suffice to reach 99% of $I_{p\text{max}}$ (15). The K^+ -channel blocker Ba^{2+} was added to the basolateral buffer to prevent local K^+ recirculation such that the ouabain-sensitive current generated by the pump would correspond to the translocation of one charge per cycle (2). The blockage of the transmembranous K^+ conductive pathways by Ba^{2+} is responsible for the low spontaneous potential difference mentioned above. Indeed, one can calculate that from the mean value of 9.7 mV given above, only 4.6 mV ($n = 28$) is due to diffusive pathways, the rest being due to the Na^+ pump activity.

In summary, the apical permeabilization with digitonin not only permits the introduction of soluble compounds into the cells but also allows the measurement of the current generated by the Na^+ pumps in situ under controlled ionic conditions. This experimental system opens possibilities to study the role of other soluble but otherwise not membrane permeant compounds in the regulation of epithelial Na^+ pump function.

Support of Na^+ pump function by glycolysis and oxidative phosphorylation. Our observation that 55% of the Na^+ pump activity was inhibited when oxidative phosphorylation was blocked with antimycin A indicates that at least one-half of the ATP used by the Na^+ pump, at near-maximal pumping rate, is provided by the mitochondria. Interestingly, inhibition of oxidative phosphorylation by antimycin A was less effectively compensated by the addition of ATP than inhibition of the glycolytic pathway. This suggests that mitochondria could preferentially provide ATP to Na^+ pumps or a subpopulation thereof. This hypothesis is in agreement with the morphological observations that mitochondria are mostly localized next to the basolateral membrane at the level of several segments of the mammalian nephron (18). However, it also could be that the pretreatment with antimycin A, which was added 30 min before permeabilization and which produced a small decrease in I_{sc} (see Table 1), induced a downregulation of Na^+ pump function that was not reversed by the addition of substrates.

Our data, which suggest that part of the Na^+ pump activity is preferentially supported by ATP produced by mitochondria, are at odds with the results obtained with A6 cells in suspension (20). In this situation, inhibition of Na^+ pump by ouabain or stimulation with nystatin preferentially modified the glycolysis and not

the oxidative metabolism. The authors suggested that this could be because of a close coupling of the glycolytic enzymes and the Na⁺ pump at the cell membrane, as reported for erythrocytes (24, 27). However, the situation of suspended A6 cells, previously grown on plastic, is not comparable with that of cells maintained in a differentiated epithelium. In particular, the number of functional Na⁺ pumps at the cell surface and the subcellular localization of mitochondria and cytosolic enzyme systems cannot be maintained in rounded, suspended cells. Together, our data and those of others mentioned above suggest the possibility that a part of the Na⁺ pump surface pool of A6 cells could be closely associated with enzymes of the glycolytic pathway. Yet another part of the cell-surface Na⁺ pumps, the expression of which would depend on epithelial differentiation, could, rather, depend on the ATP produced by nearby mitochondria. It also could be that no functionally different Na⁺ pump pools exist but that the expression of more surface Na⁺ pumps in differentiated cells creates a higher ATP demand, which can only partially be covered by the (local) glycolytic ATP production.

Role of CK system in distal nephron cells. There are different situations in which the CK system can play an important functional role for ATP delivery to ATP-consuming systems. First, PCr can represent a store and buffer of high-energy phosphate that does not affect the thermodynamically relevant ATP/(ADP × P_i) as would storage in the form of ATP. Furthermore, another advantage is the proton-buffering effect of PCr hydrolysis. Second, PCr is a convenient, intracellular carrier for the transport of high-energy phosphate from the site of ATP production to that of ATP consumption, since it diffuses more readily than ATP. This second role of the CK system depends on the appropriate subcellular localization of CK isoforms at the sites of ATP production and use (for review, see Ref. 38). The local production of ATP from ADP has a great thermodynamic advantage, since it allows for locally maintaining a high ATP/(ADP × P_i), which is a prerequisite for reactions requiring a high-energy input. This has been shown to be the case for the activity of the sarcoplasmic reticulum Ca²⁺-ATPase, which is associated with CK (29). In this case, fueling the pump with PCr is more effective than with similar concentrations of ATP (17). A preferential use of ATP produced by colocalized CK has also been reported for the plasma membrane Ca²⁺-ATPase and Na⁺ pump of different cell types (5, 12, 19, 30, 36).

In contrast, PCr is not more effective for fueling the Na⁺ pump than ATP or PEP in permeabilized A6 epithelia. In the case of glycolysis inhibition, PCr even appears to be somewhat less effective than ATP. Furthermore, PEP is as effective as PCr in conditions of oxidative phosphorylation inhibition in which it only functions as phosphagen via the pyruvate kinase and not as substrate for mitochondrial respiration. These observations could suggest that the role of the CK system in A6 cells is that of an energy store (temporal buffer) rather than that of a system designed to preferentially maintain a high ATP-to-ADP ratio next to the

Na⁺ pump. However, it should be mentioned that the presence of two different isoforms of CK in A6 cells, the cytosolic *X. laevis* type IV (B-CK) and a mitochondrial isoform (see Figs. 4 and 5), nevertheless suggests that the CK-PCr system also serves as an energy shuttle system in distal nephron cells of amphibia (spatial buffer). The large relative amount of the mitochondrial isoform indicates that the PCr stores would be preferentially generated via mitochondrial metabolism and the cytosolic CK would locally use the PCr to regenerate the ATP used by the Na⁺ pump. In this respect, it is possible that the role of the cytosolic CK isoform in providing ATP for the Na⁺ pump function has been underestimated in our study. Indeed, the leak of cytosolic CK across the permeabilized apical membrane progressively decreased its overall intracellular concentration. Furthermore, the digitonin-containing buffer might interfere with noncovalent interactions that otherwise could maintain the cytosolic CK in the vicinity of the Na⁺ pumps. The present study also shows that A6 cells contain, in addition, significant levels of adenylate kinase, another ATP-regenerating system (Fig. 4, lane 2).

The results of the present study on the expression of CK in A6 cells and its functional involvement in Na⁺ transport suggest that the CK system plays an important role as temporal and possibly spatial energy buffer in distal nephron cells. This conclusion is supported by published data showing that renal CK is localized essentially to the distal part of the mammalian nephron (10, 14), that the PCr level is higher in distal convoluted tubule than in more proximal segments, and that a brief ischemia acutely decreases that level only in the distal tubule (1). The presence of the PCr energy buffer in distal nephron cells can be related to the fact that these cells need to be able to undergo acute, high-amplitude regulatory changes in Na⁺ transport activity. In this respect, the situation of distal nephron cells resembles that of other cells with fluctuating energy requirements, such as skeletal myocytes and other cells for which the role of PCr as energy buffer is already established (36).

Finally, apically digitonin-permeabilized A6 epithelia are a useful model for further studies on the effects of exogenously added substrates, regulators, and/or inhibitors on Na⁺ pump function.

We thank Ursula Bolliger and David Frasson for the cell culture, Jacques Robert for providing the *X. laevis* CK III and IV cDNAs, Christian Gasser for the artwork, Ian Forster for reading the manuscript, and Dieter Brdiczka for fruitful discussion and suggestions.

This study was supported by Swiss National Science Foundation Grant 31-39449.93 (to F. Verrey) and by the Swiss Society for Research on Muscle Diseases (to T. Wallimann). M. L. Guerrero is the recipient of a stipend from the Swiss Government.

Address for reprint requests: F. Verrey, Institute of Physiology, Univ. of Zürich, Winterthurerstrasse 190, CH-8057 Zürich, Switzerland.

Received 17 June 1996; accepted in final form 6 September 1996.

REFERENCES

1. Bastin, J., N. Cambon, M. Thompson, O. H. Lowry, and H. B. Burch. Change in energy reserves in different segments of

- the nephron during brief ischemia. *Kidney Int.* 31: 1239–1247, 1987.
2. **Beron, J., L. Mastroberardino, A. Spillmann, and F. Verrey.** Aldosterone modulates sodium kinetics of Na,K-ATPase containing an $\alpha 1$ subunit in A6 kidney cell epithelia. *Mol. Biol. Cell* 6: 261–271, 1995.
 3. **Beron, J., and F. Verrey.** Aldosterone induces early activation and late accumulation of Na-K-ATPase at surface of A6 cells. *Am. J. Physiol.* 266 (Cell Physiol. 35): C1278–C1290, 1994.
 4. **Bertorello, A. M., and A. I. Katz.** Regulation of Na⁺-K⁺ pump activity: pathways between receptors and effectors. *News Physiol. Sci.* 10: 253–259, 1995.
 5. **Blum, H., J. A. Balschi, and R. G. Johnson.** Coupled in vivo activity of creatine phosphokinase and the membrane-bound (Na⁺/K⁺)-ATPase in the resting and stimulated electric organ of the electric fish *Narcine brasiliensis*. *J. Biol. Chem.* 266: 10254–10259, 1991.
 6. **Chang, D., and D. C. Dawson.** Digitonin-permeabilized colonic cell layers: demonstration of calcium-activated basolateral K⁺ and Cl⁻ conductances. *J. Gen. Physiol.* 92: 281–306, 1988.
 7. **De Weer, P.** Cellular sodium-potassium transport. In: *The Kidney: Physiology and Pathophysiology* (2nd ed.), edited by D. W. Seldin and G. Giebisch. New York: Raven, 1992, p. 93–112.
 8. **Esparis-Ogando, A., C. Zurzolo, and E. Rodriguez-Boulan.** Permeabilization of MDCK cells with cholesterol binding agents: dependence on substratum and confluency. *Am. J. Physiol.* 267 (Cell Physiol. 36): C166–C176, 1994.
 9. **Ewart, H. S., and A. Klip.** Hormonal regulation of the Na⁺-K⁺-ATPase: mechanisms underlying rapid and sustained changes in pump activity. *Am. J. Physiol.* 269 (Cell Physiol. 38): C295–C311, 1995.
 10. **Friedman, D. L., and M. B. Perryman.** Compartmentation of multiple forms of creatine kinase in the distal nephron of the rat kidney. *J. Biol. Chem.* 266: 22404–22410, 1991.
 11. **Gonda, T. J., D. K. Sheiness, and J. M. Bishop.** Transcripts from the cellular homologs of retroviral oncogenes: distribution among chicken tissues. *Mol. Cell. Biol.* 2: 617–624, 1982.
 12. **Hardin, C. D., L. Raeymaekers, and R. J. Paul.** Comparison of endogenous and exogenous sources of ATP in fueling Ca²⁺ uptake in smooth muscle plasma membrane vesicles. *J. Gen. Physiol.* 99: 21–40, 1992.
 13. **Hersey, S. J., and L. Steiner.** Acid formation by permeable gastric glands: enhancement by prestimulation. *Am. J. Physiol.* 248 (Gastrointest. Liver Physiol. 11): G561–G568, 1985.
 14. **Ikedo, K.** Localization of brain type creatine kinase in kidney epithelia cell subpopulations in rat. *Experientia* 44: 734–735, 1988.
 15. **Jaisser, F., P. Jaunin, K. Geering, B. C. Rossier, and J. D. Horisberger.** Modulation of the Na,K-pump function by beta subunit isoforms. *J. Gen. Physiol.* 103: 605–623, 1994.
 16. **Jørgensen, P. L.** Structure, function and regulation of Na,K-ATPase in the kidney. *Kidney Int.* 29: 10–20, 1986.
 17. **Korge, P., S. K. Byrd, and K. B. Campbell.** Functional coupling between sarcoplasmic-reticulum-bound creatine kinase and Ca²⁺-ATPase. *Eur. J. Biochem.* 213: 973–980, 1993.
 18. **Kriz, W., and B. Kaissling.** Structural organization of the mammalian kidney. In: *The Kidney: Physiology and Pathophysiology* (2nd ed.), edited by D. W. Seldin and G. Giebisch. New York: Raven, 1992, p. 707–777.
 19. **Kültz, D., and G. N. Somero.** Ion transport in gills of the euryhaline fish *Gillichthys mirabilis* is facilitated by a phospho-creatine circuit. *Am. J. Physiol.* 268 (Regulatory Integrative Comp. Physiol. 37): R1003–R1012, 1995.
 20. **Lynch, R. M., and R. S. Balaban.** Energy metabolism of renal cell lines, A6 and MDCK: regulation by Na-K-ATPase. *Am. J. Physiol.* 252 (Cell Physiol. 21): C225–C231, 1987.
 21. **Mandel, L. J., R. Bacallao, and G. Zampighi.** Uncoupling of the molecular fence and paracellular gate functions in epithelial tight junctions. *Nature Lond.* 361: 552–555, 1993.
 22. **Mandel, L. J., R. B. Doctor, and R. Bacallao.** ATP depletion: a novel method to study junctional properties in epithelial tissues. 2. Internalization of Na⁺,K⁺-ATPase and E-cadherin. *J. Cell Sci.* 107: 3315–3324, 1994.
 23. **Marjanovic, M., and J. S. Willis.** ATP dependence of Na(+)-K(+) pump of cold-sensitive and cold-tolerant mammalian red blood cells. *J. Physiol. Lond.* 456: 575–590, 1992.
 24. **Mercer, R. W., and P. B. Dunham.** Membrane-bound ATP fuels the Na/K pump. Studies on membrane-bound glycolytic enzymes on inside-out vesicles from human red cell membranes. *J. Gen. Physiol.* 78: 547–568, 1981.
 25. **Nonaka, T., and J. B. Stokes.** Metabolic support of Na⁺ transport by the rabbit CCD—analysis of the use of equivalent current. *Kidney Int.* 45: 743–752, 1994.
 26. **Payne, R. M., R. C. Haas, and A. W. Strauss.** Structural characterization and tissue-specific expression of the mRNAs encoding isoenzymes from two rat mitochondrial creatine kinase genes. *Biochim. Biophys. Acta* 1089: 352–361, 1991.
 27. **Proverbio, F., and J. F. Hoffmann.** Membrane compartmentalized ATP and its preferential use by the Na,K-ATPase of human red cell ghosts. *J. Gen. Physiol.* 69: 605–632, 1977.
 28. **Robert, J., J. Wolff, H. Jijakli, J. D. Graf, F. Karch, and H. R. Kobel.** Developmental expression of the creatine kinase isozyme system of *Xenopus*: maternally derived CK-IV isoform persists far beyond the degradation of its maternal mRNA and into the zygotic expression period. *Development* 108: 507–514, 1990.
 29. **Rossi, A. M., H. M. Eppenberger, V. Pompeo, R. Cotrufo, and T. Wallimann.** Muscle-type MM creatine kinase is specifically bound to sarcoplasmic reticulum and can support Ca²⁺ uptake and regulate local ATP/ADP ratios. *J. Biol. Chem.* 265: 5258–5266, 1990.
 30. **Saks, V. A., N. V. Lipina, V. G. Sharov, V. N. Smirnov, E. Chazov, and R. Grosse.** The localization of the MM isozyme of creatine phosphokinase on the surface membrane of myocardial cells and its functional coupling to ouabain-inhibited (Na⁺,K⁺)-ATPase. *Biochim. Biophys. Acta* 465: 550–558, 1977.
 31. **Uchida, S., and H. Endou.** Substrate specificity to maintain cellular ATP along the mouse nephron. *Am. J. Physiol.* 255 (Renal Fluid Electrolyte Physiol. 24): F977–F983, 1988.
 32. **Vandewalle, A., G. Warthensohn, H. G. Heidrich, and W. G. Guder.** Distribution of hexokinase and phosphoenolpyruvate carboxykinase along the rabbit nephron. *Am. J. Physiol.* 240 (Renal Fluid Electrolyte Physiol. 9): F492–F500, 1981.
 33. **Verrey, F.** Antidiuretic hormone action in A6 cells: effect on apical Cl and Na conductances and synergism with aldosterone for NaCl reabsorption. *J. Membr. Biol.* 138: 65–76, 1994.
 34. **Verrey, F.** Transcriptional control of sodium transport in tight epithelia by adrenal steroids. *J. Membr. Biol.* 144: 93–110, 1995.
 35. **Verrey, F., J. Beron, and B. Spindler.** Corticosteroid regulation of renal Na,K-ATPase. *Mineral Electrolyte Metab.* 22: 279–292, 1996.
 36. **Wallimann, T., and W. Hemmer.** Creatine kinase in non-muscle tissues and cells. *Mol. Cell. Biochem.* 133/134: 193–220, 1994.
 37. **Wallimann, T., T. Schlösser, and H. M. Eppenberger.** Function of M-line-bound creatine kinase as intramyofibrillar ATP regenerator at the receiving end of the phosphorylcreatine shuttle in muscle. *J. Biol. Chem.* 259: 5238–5246, 1984.
 38. **Wallimann, T., M. Wass, D. Brdiczka, K. Nicolay, and H. M. Eppenberger.** Intracellular compartmentation, structure and function of creatine kinase isoenzymes in tissues with high and fluctuating energy demands: the phosphocreatine circuit for cellular energy homeostasis. *Biochem. J.* 281: 21–40, 1992.
 39. **Wyss, M., J. Schlegel, P. James, H. M. Eppenberger, and T. Wallimann.** Mitochondrial creatine kinase from chicken brain. *J. Biol. Chem.* 265: 15900–15908, 1990.